ANALYSIS FOR NATURALLY OCCURING RADIONUCLIDES AT ENVIRONMENTAL CONCENTRATIONS BY GAMMA SPECTROMETRY

A. S. MURRAY, R. MARTEN, A. JOHNSTON, P. MARTIN

Alligator Rivers Region Research Institute, C/- Post Office,
Jabiru, N.T. 5796 (Australia)

The analytical potential of low level, high resolution gamma-ray spectrometry for naturally occurring radionuclides at environmental levels is described, with particular emphasis on detector background levels and sensitivity. Comparisons are drawn between the performance of a specially designed low background detector system, and that of standard "off the shelf" devices. Sample characteristics, calibration procedures and checks, are described, and empirical minimum detection limits of between 0.4 $Bq \cdot kg^{-1}$ (^{226}Ra, ^{228}Th) and 10 $Bq \cdot kg^{-1}$ (^{210}Pb) are derived for soil or sediment samples of about 250 g. Representative analyses of a variety of environmental samples, including water, plant material, animal tissue and sediment, are given to illustrate the routine use of the spectrometer.

Introduction

In environmental studies of the radioecology of natural series nuclides, it is desirable to obtain information not only on the behaviour of individual radionuclides of particular interest, but also on other radionuclides which may act as tracers of such phenomena as biological variability between individual organisms, variations in sediment deposition rate, or seasonal variation in concentration. One of the most powerful techniques available for this type of analysis is quantitative gamma ray spectrometry; this approach has been in use for many years. However, descriptions of such work concentrate on the analysis of particular nuclides, or even isotopes (e.g. Elsinger, et al., 1982; Michel, et al., 1981; Cutshall, et al., 1982). Few authors appear to have developed the full potential of high resolution, low level gamma spectrometry for natural series nuclides, although Smith and Wollenberg (1972) have outlined a broad analytical technique suitable for high grade materials.

To examine the potential of high resolution gamma spectrometry, consider the spectra shown in figure 1, obtained using a 19% n-type intrinsic germanium detector in a standard side arm cryostat assembly. The spectrum representing the uranium series is of a uraninite ore (BL-5, supplied by the Canadian Centre for Mineral and Energy Technology, CANMET), diluted and sealed in

100 Bq U—238 in secular equilibrium
counted for 76 ksec

100 Bq Th—232 in secular equilibrium
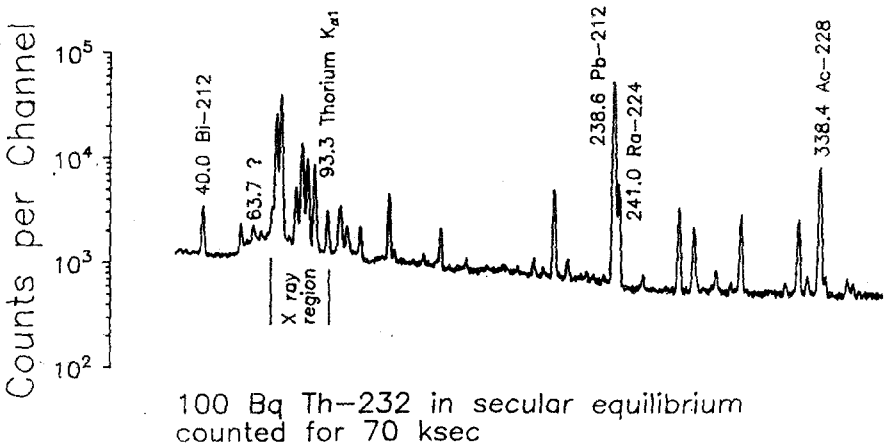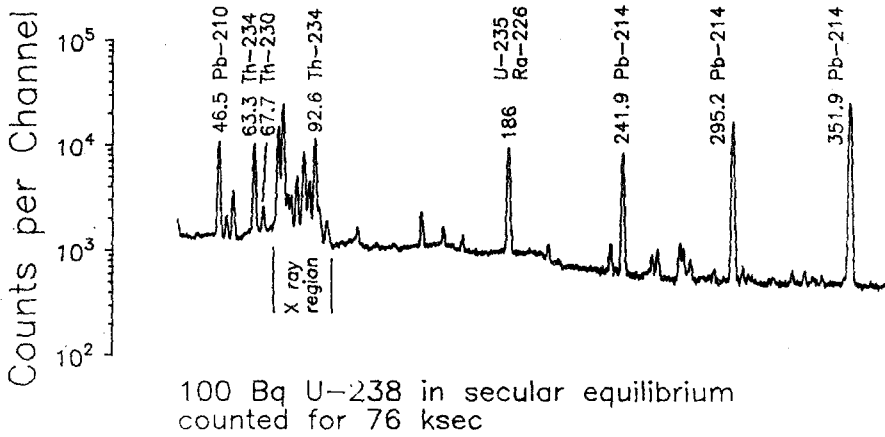counted for 70 ksec

Fig. 1. Representative spectra of high activity standards

polyester resin to minimise escape of Rn-222. The nominal 2 g sample contains
about 100 Bq (0.4%) U-238 with daughters in equilibrium. The spectrum
representing the thorium series is of aged thorium nitrate (TYS.1, supplied by
Amersham International Pty Ltd) again diluted and sealed in resin. In this
case the nominal 2 g sample contains about 100 Bq (1.2%) Th-232 with daughters
in equilibrium. Only the spectrum covering the energy range 0 to 400 keV is
shown.

Table 1
Major divisions in the uranium and thorium decay chains and associated gamma-rays

Group	Long lived nuclide	Gamma emitting nuclide	Principal associated gamma ray, keV
1	U-238	Th-234	63.3
		Th-234	92.6
		Pa-234m	1001.0
	U-235	U-235	185.7
2	U-234	U-234	53.2
3	Th-230	Th-230	67.7
4	Ra-226	Ra-226	186.0
5	Rn-222	Pb-214	241.9
		Pb-214	295.2
		Pb-214	351.9
		Bi-214	609.3
6	Pb-210	Pb-210	46.5
7	Th-232	−	−
8	Ra-228	Ac-228	338.4
		Ac-228	911.1
		Ac-228	968.9
9	Th-228	Ra-224	241.0
10	Rn-220	Pb-212	238.6
		Tl-208	583.1

It is convenient to discuss these spectra in terms of groups of radionuclides, which reflect the presumed potential for disequilibria based on half lives and physico-chemical parameters. A list of the principle radionuclides of these groups and their associated gamma rays is given in table 1. Group 1 contains

U-238 and short lived daughters and U-235. U-238 can be determined from the Th-234 lines at 63.3 keV and the 92.4 and 92.8 keV doublet, assuming secular equilibrium. This assumption is almost always valid in mineral samples, and often true in biological materials. In any case laboratory storage can be used to guarantee equilibrium. Both energy regions have interference from the thorium series, from an unassigned peak at 63.7 keV (see section 5) and from the thorium $K_{\alpha 1}$ line at 93.3 keV. There is also a weak line from P-234 at 1001.0 keV, but this is only useful in active samples. U-235 has a strong line at 185.7 keV which interferes with the only Ra-226 line. The U-235 contribution to this doublet can be independently determined by using the Th-234 lines discussed above, and assuming the U-235/U-238 activity ratio of 0.04605; this line then provides a Ra-226 determination.

Neither U-234 (group 2) or Th-230 (group 3) are strong gamma emitters. There is a weak line at 53.2 keV from U-234 with considerable interference from Pb-214 (group 5), and a line at 67.7 keV from Th-230. The latter can give some useful information at environmental levels.

Ra-226 (group 4) has a single strong line at 186.0 keV, but with U-235 interference as discussed. However, if equilibrium with Rn-222 and short lived daughters (group 5) can be assumed, then this line can be used to better effect as a means of determining U-235, and thus provide an additional analysis of group 1. There are several strong lines from group 5, particularly at 295.2 keV and 351.9 keV from Pb-214, and at 609.3 keV from Bi-214.

Finally in the uranium series Pb-210 and daughters (group 6) have one line at 46.5 keV. Unfortunately there is no gamma emission from Po-210 or daughters.

In the Th-232 series, Th-232 itself (group 7) has no gamma emission. This is usually only of concern in biological samples; in most mineral samples equilibrium between Th-232, Ra-228 and Ac-228 (group 8) can be assumed. There are several strong Ac-228 lines, particularly at 338.4, 911.1 and 968.9 keV.

Th-228 and Ra-224 (group 9) may be determined from the Ra-224 line at 241.0 keV if the interference from Pb-214 at 241.9 keV is taken into account. If equilibrium with group 10 (Rn-220 and daughters) can be assumed, a more accurate determination is available from the Pb-212 peak at 238.6 keV and the Tl-208 peak at 583.1 keV.

Experimental

Typical High Resolution Spectrometer

A typical spectrometry system is shown diagramatically in figure 2. The
electronic processing is self explanatory, although careful consideration
should be given to amplifier selection. Optimum resolution at low count rates
is not necessarily obtained by using an apparently high performance amplifier,
as resolution is often compromised to produce constant (rather than optimum)
performance at varying count rates. In analysing environmental samples high
count rates are not encountered, and we have found that more economical
amplifiers often give better performance. The specifications for the n-type
detector are given in table 2, and some comments are in order.

(a) Resolution — Some improvement, especially at low energies, is
available here; 800 eV at 122 keV is now routinely obtainable for
a crystal of this size.

(b) Efficiency — in environmental work, this figure is of less value
than the absolute efficiency curve, given in figure 3, curve A.
This curve was obtained using our standard disc geometry discussed
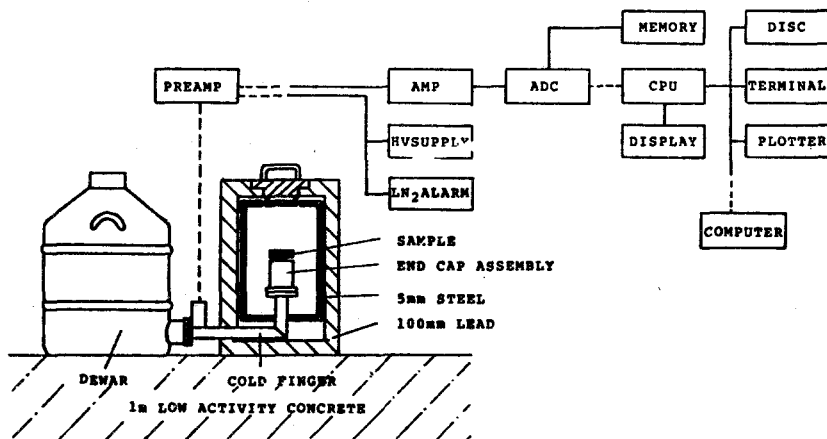in section 3. Note that the efficiency performance at low

Fig. 2. Typical spectrometer assembly

267

Table 2
Characteristics of detector

Manufacturer: Canberra

Material: n—type intrinsic germanium

Geometry: Reverse electrode closed end coaxial

Resolution: 1.83 keV FWHM at 1.33 MeV
             3.37 keV FWTM
             peak to Compton 50.5:1
             1.07 keV FWHM at 122 keV

Efficiency: 19.2% relative to a 3" by 3" NaI crystal
             25 cm source to detector distance

Physical Characteristics:
                 Diameter: 43.9 mm
                 Length: 55 mm
                 Detector to window: 5 mm approx
                 Window: 500 μm Beryllium

energies decreases only slightly, mainly due to sample self
attenuation. However, the efficiency curves shown of the 3 p—type
detectors decrease rapidly at low energy, because of attentuation
by the insensitive germanium layer forming the outer electrode.
The end cap windows in these three detectors are all about 0.5 mm
of aluminium, which only attenuates 46 keV photons by 5%. Thus
the variation in low energy sensitivity arises from variations in
the thickness of the germanium dead layer.

(c) Background — this is the specification that has received almost no
attention from most of the major manufacturers until very
recently, (Malm et al., 1984; Zimmer and Wagner, 1984). The
detector background can be considered as made up of an internal
and an external component but for an existing detector only the
latter can be optimised (usually against cost); 100 mm of lead
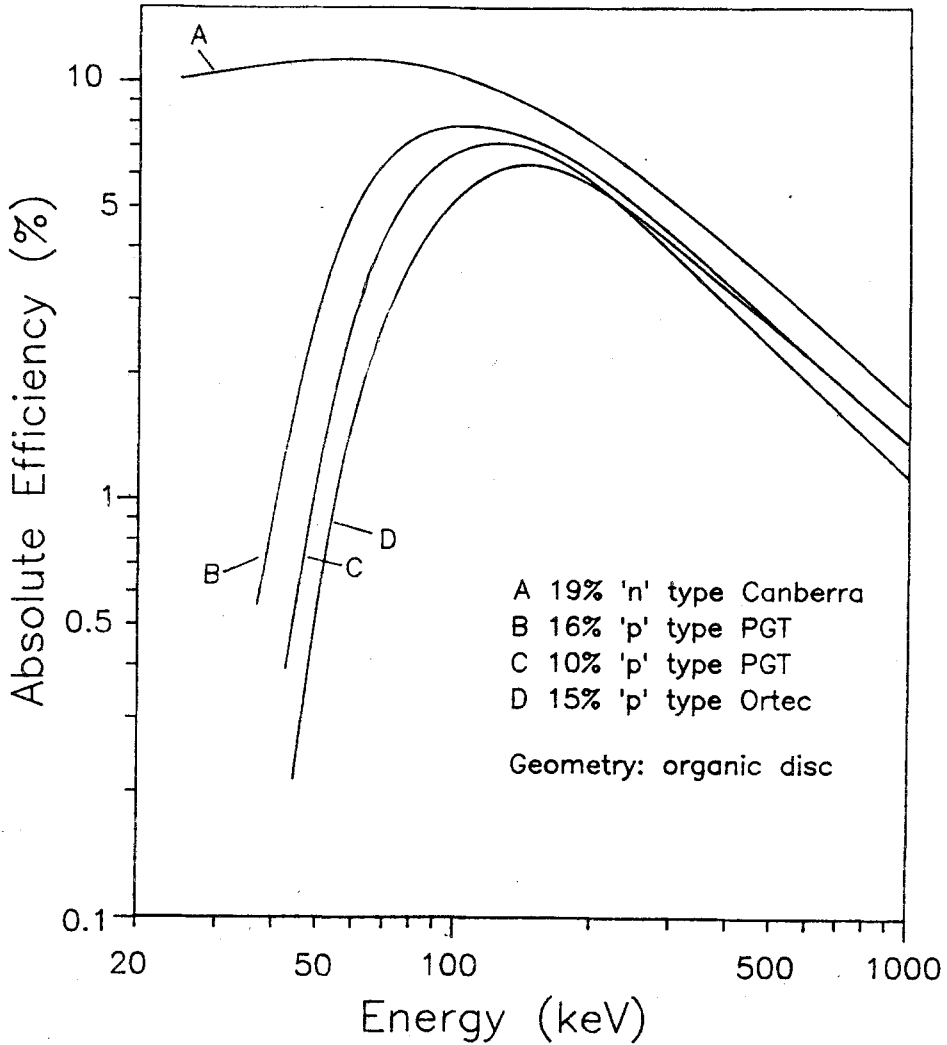
Fig. 3. Absolute efficiency curves for four detectors

lined with 5 to 10 mm of steel or copper is usually considered
adequate to attenuate high energy X-rays stimulated in the lead
and to attenuate Pb-210 photons from the shield. The lead, steel
and copper should all be selected for low inherent activity;
suitably low levels are easily achieved. If possible, attention
should be paid to the building surrounding the detector. Our

shielded detectors are housed in a metal/fibro-cement clad building, constructed on about 1 metre of selected low activity concrete. The effects of a more conventional laboratory may be twofold; greater external gamma flux giving a higher count rate inside the lead shield, and increased Rn-222 (and daughters) concentration in the laboratory atmosphere. The latter can be overcome locally by displacement with an aged gas (air, nitrogen).

Using such selected low background shielding, it became clear that, in all cases we encountered (four conventional off the shelf detectors), background spectra were dominated by discrete lines at the energies of interest arising from within the detector assemblies. Bartels (1980) and Wogman (1981) have considered natural series contamination in a variety of materials suitable for use in the construction of cryostat assemblies, and others have considered the problem of the natural series contribution to detector background (e.g. Cooper and Perkins, 1972; Camp et al, 1974, Murray and Aitken, 1980). With these data in mind, we commissioned Canberra to build the cryostat to our specification. Aluminium was avoided, extensive use being made of magnesium and copper, and the cryostat molecular sieve, a source of radon daughters, was replaced with activated charcoal. A beryllium window was specified to permit low energy x-ray analysis. However, beryllium frequently contains uranium and in our case the only significant natural lines in the background spectrum are from U-238 and short lived daughters. We have decided to replace the window with one of magnesium alloy as soon as possible. This will have a negligible effect on the sensitivity at 46 keV.

The background observed using this custom made detector within an enclosure of 100 mm of lead and 5 mm of steel is compared with the background of a 16.5% p-type detector in figure 4. The latter is manufactured by P.G.T. in a similar side arm cryostat to that made by Canberra, but with little attention paid to the activity of materials used.
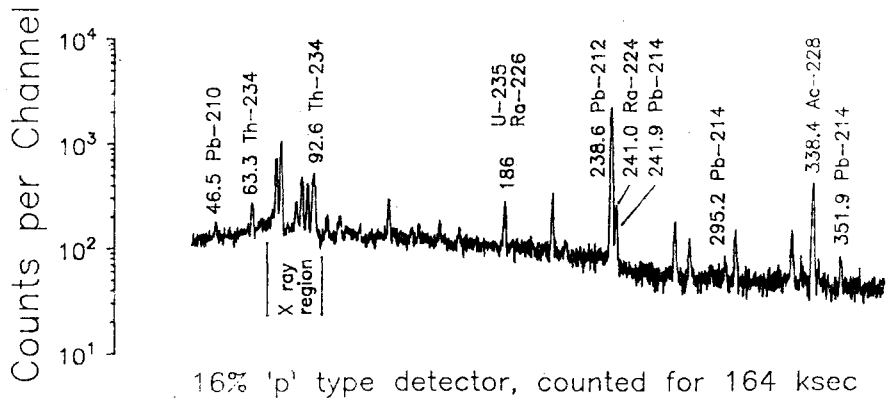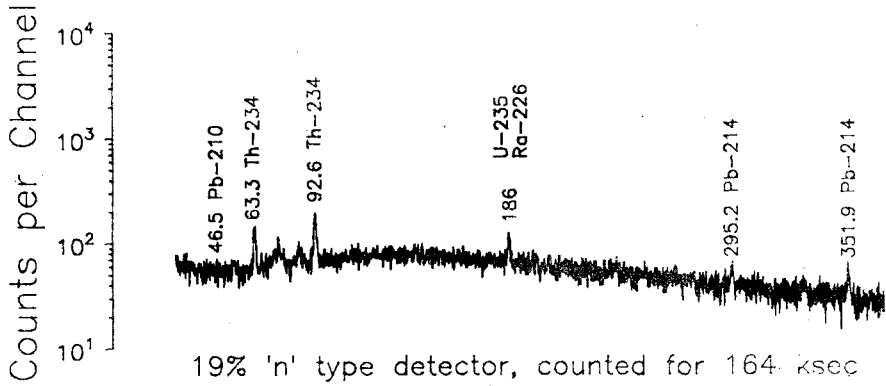
Fig. 4a. Background spectra taken in 5 mm steel and 100 mm lead

The count rates observed in the peaks in four detectors in a
similar shield assembly are given in table 3. The variation from
one detector to another is considerable and can be more readily
seen in figure 5, where the count rates of some of the main peaks
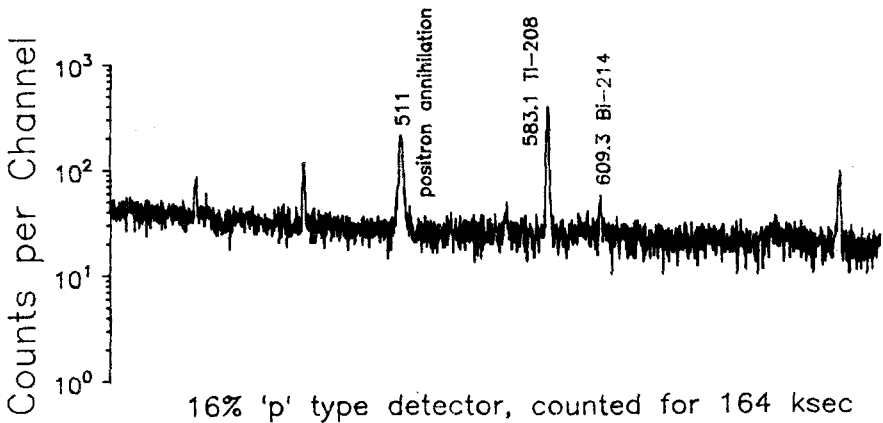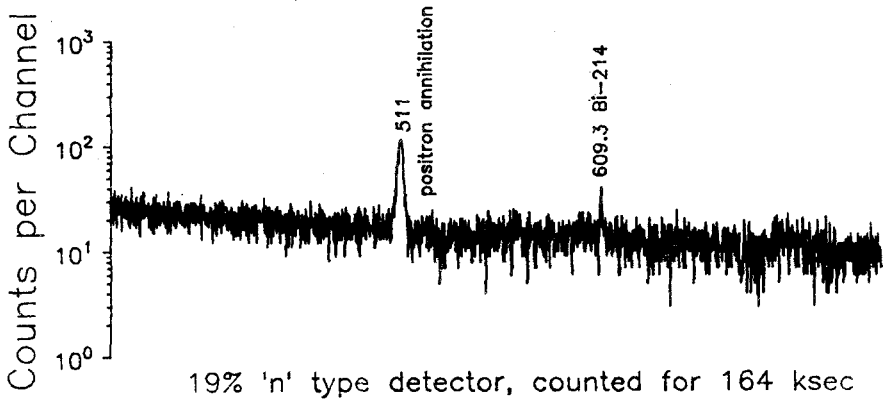are given as a ratio to those of the Canberra n-type.

271

19% 'n' type detector, counted for 164 ksec

16% 'p' type detector, counted for 164 ksec

Fig. 4b. Background spectra taken in 5 mm steel and 100 mm lead

Sample Presentation

Any sample presentation technique must meet several requirements, such as
reproducible geometry, ease of preparation and reliable radon retention. Our
approach to this problem has been to prepare all samples (minerals or ashed
biological material) as a fine homogeneous powder by ring grinding. This
powder is then cast using polyester resin in one of three moulds of 33 cm^3,
201 cm^3 and 1025 cm^3, illustrated in figure 6. Typically, sample preparation
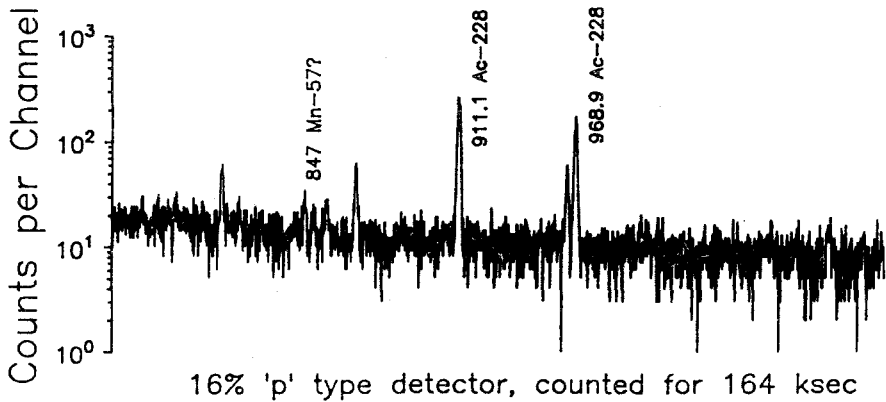time using ground material is about 15 minutes, and the maximum sample
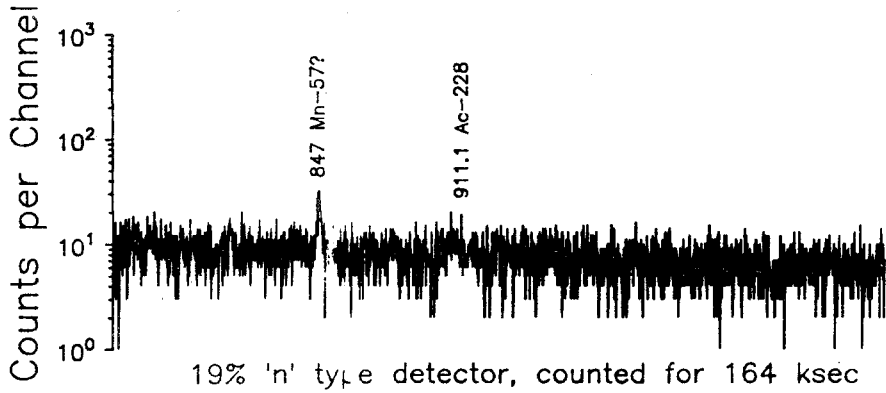
Fig. 4c. Background spectra taken in 5 mm steel and 100 mm lead

proportion in the mould is about 70%. This gives mineral sample weights of
40 g, 250 g, and 1.3 kg respectively, and biological (ash) sample weights of
about half these values. When there is insufficient sample to load the mixture
to this value, the balance is made up with solid resin powder (ground to less
than 150 μm). This minimises settling of the sample during curing of the
resin and the resulting uncertainties in homogeneity. This is especially
important with biological ash, when there may only be a few grams of sample
available. It has been shown using a mineral sample of 7 cm^3 that this
casting process reduces the radon loss from approximately 20% in the loose

273

Fig. 4d. Background spectra taken in 5 mm steel and 100 mm lead
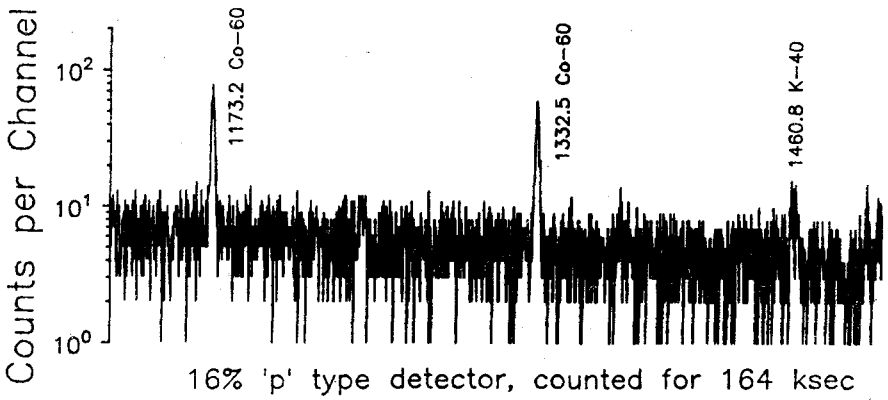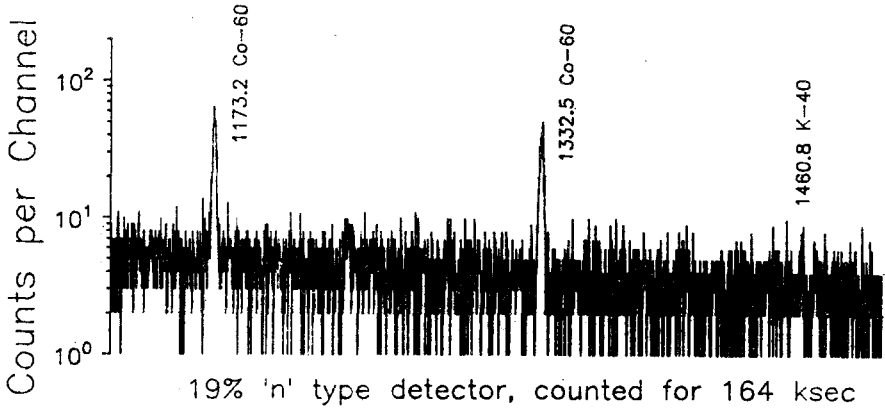
sample to less than 0.3% (Murray, 1981). For these geometries with a much
smaller surface to volume ratio, the retention factor should be even
greater. Typical absolute efficiency curves for these geometries are given in
figure 7.

Table 3
Background peak count rates for four detectors

Parent	Nuclide	Energy keV	A ksec^{-1}	B ksec^{-1}	C ksec^{-1}	D ksec^{-1}
U-238	Th-234	63	3.7$_3$	5.2$_2$	1.96$_3$	2.2$_3$
Th-230	Th-230	67	0.2$_2$	0.6$_1$	0.22$_{22}$	0.3$_3$
Ra-226	Ra-226	186	2.3$_3$	5.7$_1$	2.97$_{26}$	2.4$_3$
Rn-222	Pb-214	295	1.0$_2$	1.0$_1$	0.79$_{17}$	1.4$_3$
		352	1.2$_2$	1.8$_1$	0.81$_{16}$	2.8$_3$
	Bi-214	609	0.85$_{16}$	1.3$_1$	0.90$_{10}$	2.06$_{18}$
Pb-210	Pb-210	46	0.3$_3$	1.8$_1$	0.5$_2$	2.05$_4$
Ra-228	Ac-228	338	0.2$_2$	14.5$_1$	0.58$_{16}$	0.2$_2$
		911	0.27$_{12}$	12.5$_1$	0.53$_8$	0.50$_{13}$
		969	0.2$_2$	7.2$_1$	0.18$_9$	0.23$_{10}$
Rn-220	Pb-212	239	0.4$_3$	71.8$_6$	2.25$_{21}$	9.4$_4$
	Tl-208	583	0.45$_{14}$	15.0$_2$	0.52$_{10}$	2.88$_{14}$
K-40	K-40	1461	0.30$_8$	0.64$_2$	0.48$_6$	−
Cs-137	Ba-137^M	662	0.13$_{13}$	0.180$_{10}$	0.08$_8$	0.22$_{13}$

Note: 1/   A — 19% Canberra, counted for 216 ksec;
              B — 16.5% PGT, 202 ksec; C — 10% PGT, 256 ksec;
              D — 15% ORTEC, 195 ksec.

         2/   Errors are in the least significant figures.

Sample Self Attenuation

The variation in self attenuation from sample to sample dictates the number of
different calibration standards that are needed. This variation can arise
from two sources; variations in bulk density of the sample/resin mixture with
resulting variations in the bulk attenuation coefficients, and variations in
sample mass attenuation coefficients.

After casting, bulk densities are typically 2.15 g cm^{-3} for mineral samples
and 1.50 g cm^{-3} for biological samples, with variations of only about 4% about
these values. Simple linear weight normalisation is sufficient to remove this
source of variability; it is not necessary to include the exponentially
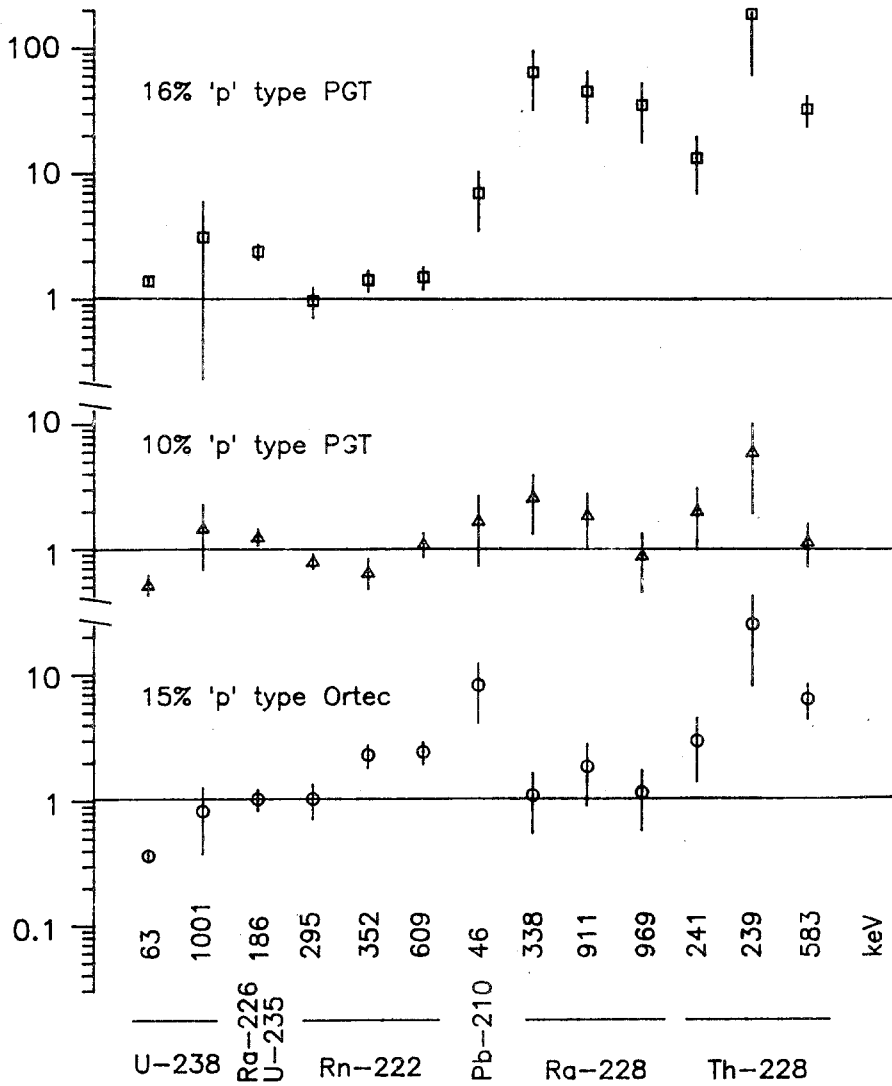
Fig. 5. Ratios of background peak intensities to those of a 19% "n" type detector

varying attenuation factor due to bulk density variations as this effect is usually negligible. It is estimated to be a maximum of 3% at 46 keV decreasing to 2% at 63 keV for mineral samples and less for biological samples. This essentially constant bulk density is a direct result of the casting process. Previous work with ground mineral samples packed into a

Volume = 33 cm³

Volume = 201 cm³

Volume = 1025 cm³
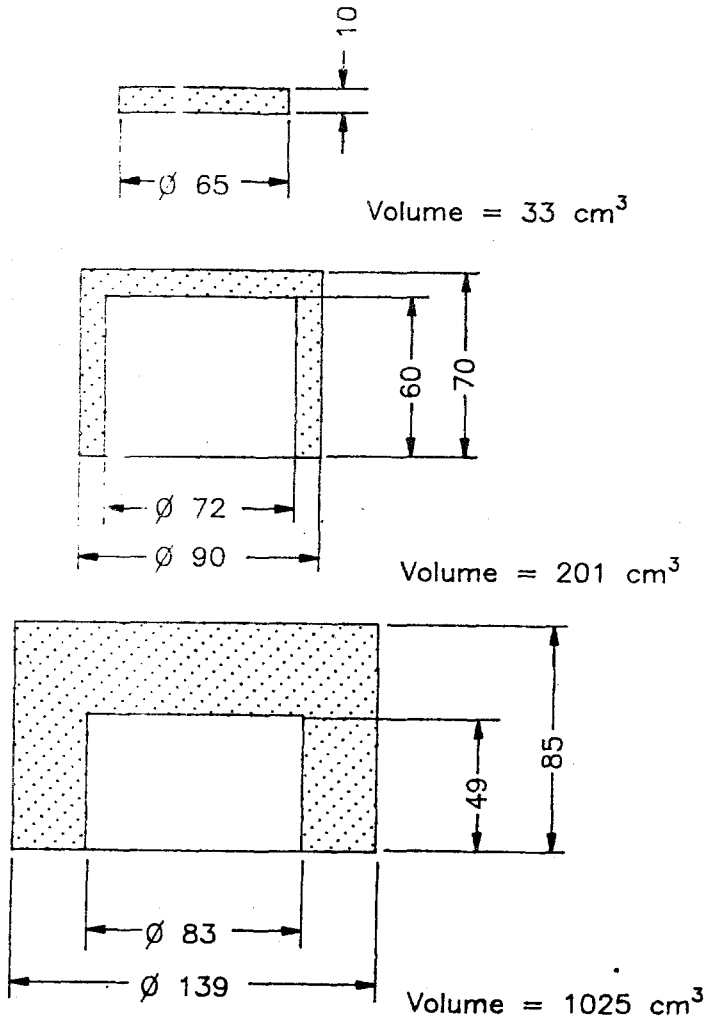
Linear dimensions in (mm)

Fig. 6. Cross section of sample moulds

Fig. 7. Absolute efficiency curves for three sample geometries

constant volume using a ram resulted in variations in bulk density of up to 30%, with additional exponential corrections of 10% at 46 keV.

The other contribution to variability in sample self attenuation is from the variation in sample mass attenuation coefficients. This is reduced by the effective dilution of variability in the constant characteristics of the
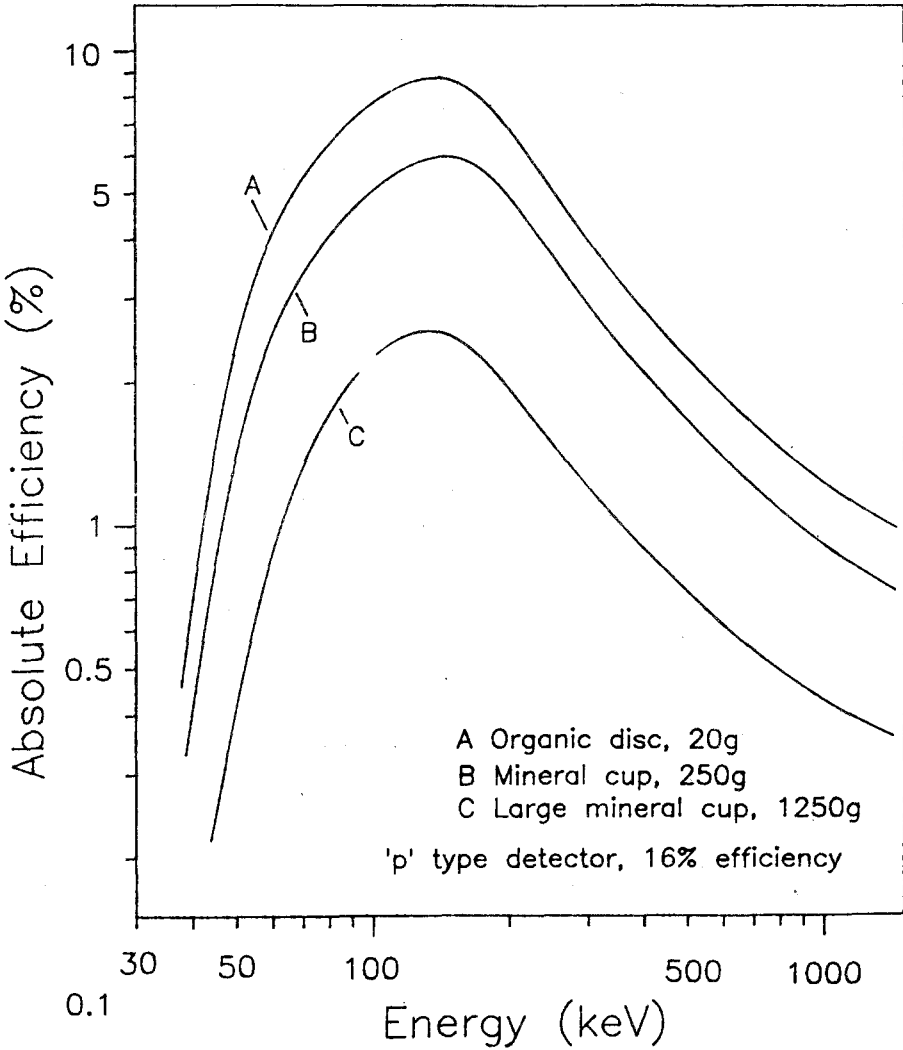
278

resin. We have demonstrated experimentally that the difference in self
attenuation characteristics between a pure resin sample (doped with about 0.2g
of 7% uranium ore grade sand) and a disc loaded with 15 g inactive ashed
animal muscle (similarly doped) is less than 2% at 46 keV. Thus it is
concluded that variations in the ash characteristics are unlikely to have
significant effect.

However, the same is not true for mineral samples. For minerals containing
medium and heavy elements at typical environmental concentrations it is
estimated that the likely range in mass attenuation coefficients will be
approximately 20%. This would give rise to variation of about ±10% in Pb-210
analyses. Some confirmation of the likely magnitude of this effect is given
by the observed ratio of our Pb-210 calibration data for the mineral and
biological disc geometries, where the result for the organic standard (i.e.
pure resin disc) is only 17% higher than that for the mineral (38% resin and
62% mineral) standard, after weight normalisation. Nevertheless it is
acknowledged that a ±10% uncertainty from one mineral sample to another is
unacceptable and a direct routine method of measuring the attenuation
characteristics of each disc, similar to that of Cutshall, et al (1983), is
under development.

Calibration

Some authors (eg. Momeni, 1982) suggest the use of absolute emission
intensities in conjunction with a well defined efficiency curve for the
calibration of detectors for use at environmental concentrations. However,
for the analyses described here, this is not straight forward. Several
radionuclides in the natural decay chains emit photons in cascade (e.g.
Pb-214, Bi-214, Ac-228), and if samples containing these nuclides subtend a
large solid angle at the detector (as is usually arranged to be the case for
samples of low activity), then there is a high probability of recording sum
events and thus removing counts from the photo-peak. Although in principle
these summation problems can be corrected for (eg. Debertin and Schötzig,
1978) this is complex, and provides an additional source of error. The
alternative approach used here of direct calibration using standard sources is
easier and capable of great accuracy.

Calibration of the spectrometer depends on comparison with standards of
similar attenuation characteristics. Some separation of the groups described

in section 1 is necessary because of interference, particularly at 186 keV between U-235 and Ra-226, and at 63 keV between Th-234 and the unknown line from group 8 (Ra-228 and Ac-228) in the thorium series. This line was first identified with this group, rather than with uranium series contamination or with group 9 (Th-228) by Murray (1981) but no attempt has been made to confirm that it did not originate from Th-232 (group 7).

(a)   Uranium series standards - These are all based on the CANMET uraninite ore EL-5. The concentrations of total uranium and Ra-226 are certified by CANMET, and they produce evidence that Pb-210 is in equilibrium with Ra-226. This material is diluted by weight in an inactive river sand ground to less than 150 μm, or in solid resin also ground to less than 150 μm. These dilute powders of known specific activity are then cast in the appropriate mould and stored for at least five half lives of Rn-222 before counting. From a consideration of mass attenuation coefficients the effect of the small quantity of ore material (typically 0.5% by weight) on the characteristics of the test matrix is negligible (less than 0.5% at 46 keV in the pure resin matrix). It has also been confirmed that the ore powder remains uniformly distributed throughout the resin matrix by comparison of the Pb-210 count rate at 46 keV from the cast disc when inverted with that when in normal configuration. The results were indistinguishable within a statistical error of about 3%.

At least three such standards have been independently prepared from each of the inactive matrices, for the two geometries in regular use (33 cm^3 disc and 201 cm^3 cup) and one mineral standard for the large volume cup.

(b)   Ra-226 standard - To separate the Ra-226 contribution to the 186 keV peak from that of U-235 a separate measurement of groups 4 and 5 (Ra-226 and Rn-222 with short lived daughters) is needed. We have used a radiochemically pure Ra-226 solution (provided by the Australian Atomic Energy Commission). A quantity of this solution was evaporated to dryness on the appropriate ground matrix, and the powder then homogenised before casting. As relative peak intensities rather than absolute values are

required, only one such source was prepared from each matrix for
each of the smaller geometries, and one mineral matrix in the
larger cup geometry. These standards were again stored for at
least five Rn-222 half lives.

The use of these standards enables the measurement of the ratio of
the intensity of the 186 keV line of Ra-226 to that of each of the
radon daughter lines at 242, 295 and 352 keV. With this procedure
the concentration of Ra-226 in any sample may be obtained by using
the radon daughter lines. After subtraction of the Ra-226
contribution, the intensity of the 186 keV line then yields the
U-235 concentration.

(c)   Th-232 series standards – These are all based on thorium nitrate
        $(Th(NO_3)_4 \cdot 4H_2O)$ supplied by Amersham International. This material
        was last processed in 1906, and all daughters down to Rn-220 will
        be in equilibrium with the parent. Lawrence (1978, private
        communication) of Amersham International has given an undated
        spectrographic analysis which indicates no elemental impurity of
        concentration greater than 25 ppm. In addition the thoria (ThO_2)
        content was found to be 47.5% which corresponds to 41.7% thorium,
        as compared with 42.03% calculated from the formula. It is thus
        assumed that the salt is stoichiometric. This salt was lightly
        crushed in an agate mortar and dispersed in the usual manner.
        Once cast in resin to retain radon, the entire thorium series is
        in equilibrium.

(d)   Other standards – In addition to the above, K-40 standards have
        been prepared using potassium sulphate and potassium chloride cast
        in resin, and Cs-137 standards using a standardised solution
        supplied by Amersham International. The latter was handled
        quantitively in a manner similar to that described above for
        Ra-226.

Typically, for each sample geometry and sample type (i.e. organic or mineral)
approximately five separate calibration standards were prepared. The standard
deviation of the distribution of the calibration factors obtained using these
different standards was about 1.5%. As a result, overall uncertainties in our

calibration data (including systematic effects) are estimated to be not more than 3% when the random component in the error on the mean is expressed at the two sigma level. The averaged calibration data for the organic standards obtained using the disc geometry on the 19% Canberra n-type detector and for the mineral standards obtained using the small and large cup geometries on the 19% Canberra n-type and the 16.5% PGT p-type detector respectively are summarised in table 4.

Table 4
Summary of calibration data for three geometries

Parent	Nuclide	Energy keV	Disc, 33cm^3 ksec^{-1}/Bq g^{-1}	Cup, 201cm^3 ksec^{-1}/Bq g^{-1}	Cup, 1025cm^3 ksec^{-1}/Bq g^{-1}
U-235	U-235	186	40.8_{15}	373_5	586_{20}
U-238	Th-234	63	84.6_6	367_4	439_{15}
Th-230	Th-230	67	9.1_4	44.0_{21}	54_{12}
Ra-226	Ra-226	186	59.6_{11}	523_6	853_{20}
Rn-222	Pb-214	295	191_4	1777_{18}	2913_{60}
	Pb-214	352	312_6	2953_{30}	4837_{98}
	Bi-214	609	196_3	1940_{20}	3447_{70}
Pb-210	Pb-210	46	91.9_6	230_3	105_{10}
Ra-228	Ac-228	338	93.5_{18}	875_9	1489_{31}
	Ac-228	911	81.4_{18}	800_8	1457_{30}
	Ac-228	969	48.4_9	467_5	860_{18}
Th-228	Pb-212	239	557_7	4825_5	8059_{162}
	Tl-208	583	131_3	1269_{13}	2360_{48}
K-40	K-40	1461	25.0_2	–	453_{10}
Cs-137	Ba-137^m	662	386_5	3650_{46}	7090_{150}

Note: 1/ The disc calibration refers to the organic disc, and is normalised to a sample weight of 20 g, the small cup to a 250 g mineral sample, and the large cup to a 1250 g mineral sample.

2/ Errors are in the least significant figures, and are two standard errors from between 3 and 7 independently prepared standards. See text for systematic errors.

3/ The 33 cm^3 organic disc and 201 cm^3 mineral cup data were derived using the 19% Canberra n-type detector. The 1025 cm^3 cup data were derived using the 16.5% P.G.T. p-type detector.

Table 5
Testing of calibration data using NBL standards

Parent	NBL 7-A $Bq \cdot g^{-1}$	NBL 42-1 $Bq\ g^{-1}$
U-238	47	496_{11}*
Th-230	–	401_{101}
Ra-226	43_4	495_4
Pb-210	–	442_{17}*
Ra-228	353_5	–
Th-228	350_6	–

Ratio to NBL certified values:

Uranium	1.01_8	0.99_2
Thorium	1.02_2	–
Ra-226[1]	–	0.97

Note: 1/   NBL do not certify the Ra-226 value, their result is given for guidance only.

2/   Those values marked * are the mean of two determinations.

3/   Errors do not include the calibration systematic uncertainties although the NBL values used did include all error components. Errors are in the least significant figures.

To provide an independant check on the reliability of these data, two standardised ores supplied by the U.S. Department of Energy, New Brunswick Laboratory, were diluted in inactive sand in the usual way and cast in the disc geometry. The results of these analyses, and the ratios of the observed parent activities to those expected, are given in table 5. It can be seen that the agreement is within experimental error for both U-238 and Th-232.

Minimum Detection Limits

It is not easy to define an unambiguous minimum detection limit in gamma spectrometry, because the background continuum is dependent on sample type and on other radionuclides present. Nevertheless, it is recognised that when

deciding in advance on an appropriate analytical technique to determine some aproximately known radionuclide activity, an estimate of a minimum detection level is useful. These levels have been derived empirically for the geometries used here using mixed uranium/thorium standards of equal known activity. These active standards were counted for various short periods of time (100 to 2000 sec) and each spectrum was then added to a background count of 77 ksec (about 21 hours). A plot of the error appropriate to each nuclide, after weighted averaging of all peaks contributing to that analysis, was obtained as a function of effective activity. This effective activity was given by the active standard count time divided by the total co·   ⸴ (i.e. sum of 77 ksec and active standard count time) and multiplied by the actual parent activity in the standard. The nuclide activity was then read off the curve at the value corresponding to a standard error of 30%. This corresponds to about a 99% certainty that the value is greater than zero. These curves are illustrated in figure 8 for the smaller mineral cup geometry. Table 6
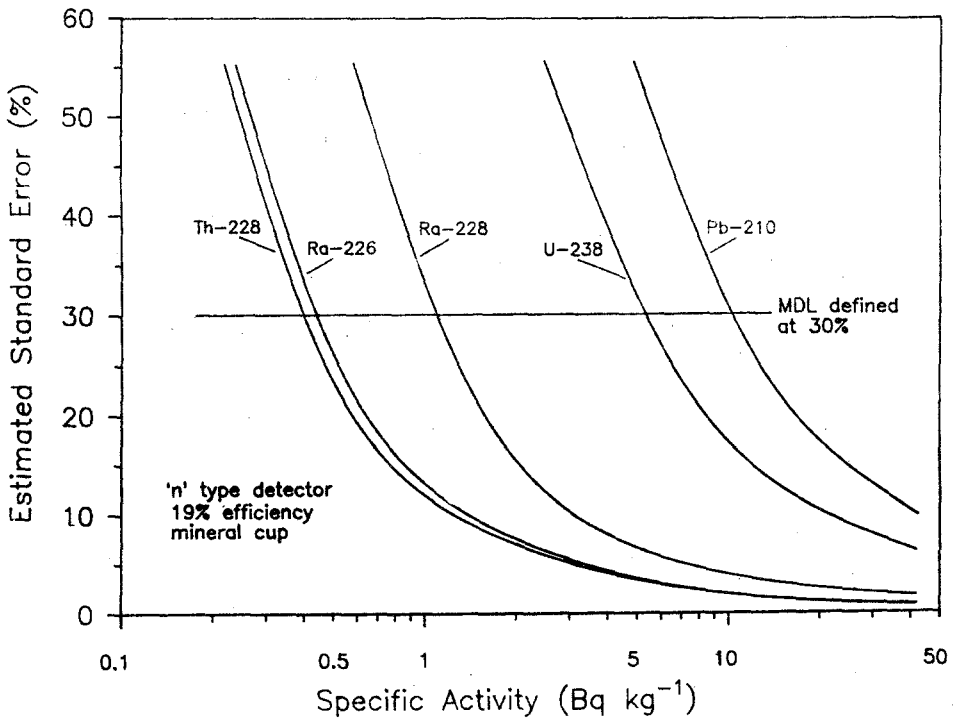

Fig. 8. Statistical counting error vs. specific activity

Table 6
Experimentally derived minimum detection limits

Nuclide	Disc, 33 cm^3 Bq kg^{-1}	Cup, 201 cm^3 Bq kg^{-1}
U-238	15	5
Ra-226	2	0.4
Pb-210	14	10
Ra-228	5	1
Th-228	2	0.4

Note: 1/ Minimum detection limit defined as that specific activity likely to
        have an associated standard error of 30%.
      2/ Data obtained with both uranium and thorium series present in
        equilibrium in a nominal 40 g mineral sample (disc geometry), and in
        a nominal 250 g mineral sample (cup geometry).
      3/ Data obtained with 19% n-type (Canberra).

summarises the minimum detection limits derived from this process for the two
smaller geometries in common use, both derived for the 19% Canberra n-type
detector.

Illustrative Analyses

Seven representative analyses are presented in Table 7. These cover a range
of specific activities from a few milliBecquerels per kg (waters) to
Becquerels per gram (mussels). These samples are briefly discussed below.

Creek waters - two 100 l samples collected simultaneously, one filtered
    through a 0.45 μm cartridge filter. Both samples were then acidified to
    1% with 'Analar' grade nitric acid and the uranium and thorium series
    radionuclides precipitated with MnO_2. This precipitate was recovered by
    filtering through Whatmans no. 42 ashless, the filter papers ashed and
    the MnO_2 recovered quantitatively. This was then cast in a disc mould in
    the usual way. Total operator time was about three hours per sample,
    with up to four samples handled simultaneously.

285

Table 7
Illustrative analyses of various types of samples

Sample	U-238	Th-234	Ra-226	Pb-210	Ra-228	Th-228	K-40	Cs-137	Sample size (wet wt)	Detector
Creek water (total)	—	3.6_8	7.2_{20}	6.4_{12}	2.0_4	1.5_2	8.7_{13}	—	84 l	A
Creek water (filtered)	—	1.9_9	6.7_{22}	2.7_{13}	1.1_5	0.44_{18}	6.5_{15}	—	78 l	A
Floodplain grass Pseudoraphis Spinescens	1.5_{10}	—	4.0_2	19.0_{10}	2.5_3	1.68_{14}	133_3	1.01_{12}	1 kg	A
Billabong – floating vegetation mat Salvinia molesta	17_3	—	73.0_{11}	82_3	37.3_{13}	21.9_6	—	2.4_3	1.1 kg	A
Billabong – algae and epiphytes	25_{10}		67.0_{14}	253_{35}	36_4	32_2	26_4	4.7_6	130 g	B
Freshwater mussels, 16 years old	<200	—	3521_{50}	895_{90}	489_{35}	549_{17}	—	—	13 g	A
Floodplain core, 9 – 12 cm	46_6	—	42.9_8	68_{24}	35.2_{19}	33.1_{10}	77.1_5	—	114 g	B

Note: 1/ Activities in Bq/kg dry weight, except waters in mBq/l.
2/ Detector code is given in Table 3. Errors are statistical only, in the least significant figures.

Flooplain grass - collected during dry season in its non-aquatic form. Dried
and then ashed at 400°C for about 4 hours, and cast in disc geometry.

Vegetation mat from Island billabong - an exotic weed which has recently
appeared on local floodplain waterways. This sample is remarkable in
that these plants are thought unlikely to be more than three months old,
and this suggests a very rapid uptake of activity. As they do not root
in the sediment, but float in dense mats on the surface, all the activity
has been removed directly from the water column. The sample was dried
and ashed as above and then cast in the disc geometry.

Algae and epiphytes - again these organisms are not likely to be more than a
few weeks old, and again they have no direct contact with the soil. They
either float free, or are attached to the stems and leaves of aquatic
plants. This material was again dried and ashed, and cast in the disc
mould.

Freshwater mussels - it is known that these mussels accumulate radium and we
have evidence to suggest that the biological half life is greater than 6
years. A bulked sample of about 10 mussels was dried and ashed, and cast
as a disc.

Floodplain core - such sedimentary materials are simply dried, homogenised and
cast, usually in the small cup geometry.

Conclusion

Even with standard high resolution detectors, gamma spectrometry is a very
useful tool in the analysis of natural radionuclides at environmental
concentrations. However, background spectra reveal significant contamination
of such detectors by natural radionuclides and we have demonstrated that if
attention is paid to detector type and end cap assembly design, particularly
in respect of the materials used, a significant increase in sensitivity is
available, especially at low energies.

With care, calibration standards can be prepared which provide typical errors

287

on calibration data of about 3%. Because of the sensitivity of the technique,
these 3% errors limit the ultimately achievable errors, especially in
biological samples where uncertainties in sample self attenuation are
negligible.   -

                                              *

References

 1. O. G. BARTELS, Health Phys., 38 (1980) 89.
 2. D. C. CAMP, C. GATROUSIS, L. A. MAYNARD, Nucl. Instr. Methods, 117 (1974) 189.
 3. J. A. COOPER, R. W. PERKINS, Nucl. Instr. Methods, 99 (1972) 125.
 4. H. H. CUTSHALL, I. L. LARSEN, C. R. OLSEN, Nucl. Instr. Methods, 206 (1983) 309.
 5. K. DEBERTIN, U. SCHÖTZIG, Nucl. Instr. Methods, 158 (1978) 471.
 6. R. J. ELSINGER, P. T. KING, W. S. MOORE, Anal. Chim. Acta, 144 (1982) 277.
 7. H. L. MALM, M. M. WATT, I. BOSTOCK, J. L. CAMPBELL, P. JAGAM, J. J. SIMPSON, Nucl. Instr. Methods,
    223 (1984) 420.
 8. J. MICHEL, W. S. MOORE, P. T. KING, Anal. Chem., 53 (1981) 1885.
 9. M. H. MOMENI, Nucl. Instr. Methods, 193 (1982) 185.
10. A. S. MURRAY, Environmental radioactivity studies relevant to thermoluminescence dating. D. Phil, Thesis,
    University of Oxford, 1981.
11. A. S. MURRAY, M. J. AITKEN, The measurement and importance of radioactive disequilibria in TL samples,
    in: A Specialist Seminar on Thermoluminescence Dating, PACT, 6 1980, p. 155.
12. A. R. SMITH, H. A. WOLLENBERG, High resolution gamma-ray spectrometry for the laboratory analysis of
    the uranium and thorium decay series, in: The Natural Radiation Environment II, J. A. S. ADAMS, W. M.
    LOWDER, T. F. GESSELL, (Eds), CONF-720805, Washington, D. C., 1972.
13. N. A. WOGMAN, Natural contamination in radionuclides detection system IEEE Trans. Nucl. Sci., (1981) 275.
14. W. H. ZIMMER, S. E. WAGNER, Nucl. Instr. Methods, 223 (1984) 412.